



Synthesis of monodisperse CdS nanowires and their photovoltaic applications

Lifei Xi^a, Winnie Xiu Wen Tan^a, Kee Sze Chua^a, Chris Boothroyd^b, Yeng Ming Lam^{a,*}

^a School of Materials Science and Engineering, Nanyang Technological University, Singapore

^b Center for Electron Nanoscopy, Technical University of Denmark, DK-2800 Kongens-Lyngby, Denmark

ARTICLE INFO

Available online 20 February 2009

Keywords:

Nanowires
Monodisperse
Cadmium sulphide
Solution process
Interconnected network

ABSTRACT

Cadmium sulphide (CdS) nanowires with a monodisperse diameter of 3.6 nm and an aspect ratio of 10–170 were successfully synthesized using a simple and reproducible hot coordinating solvents method. The morphology and optical properties of the CdS nanocrystals were investigated using transmission electron microscopy (TEM), high-resolution TEM (HRTEM) ultraviolet–visible (UV–Vis) absorption spectroscopy and photoluminescence (PL) spectroscopy. It was found that using a long alkyl chain phosphonic acid–octadecylphosphonic acid (ODPA) causes a low diffusion rate and low reactivity which help to control the morphology of the nanocrystals. The timing of the injection process was also found to have critical effect on the morphology of the nanocrystals. Sharp peaks in both the UV–Vis absorption and PL spectra indicate that the size distribution of the diameter is nearly monodisperse. The photovoltaic properties of photovoltaic devices made with a blend of our nanowires and poly[2-methoxy-5-(2'-ethyl-hexyloxy)-1,4-phenylene vinylene] (MEH-PPV) were also investigated. Devices made with the nanowires were found to have double the I_{sc} observed in devices made with lower aspect ratio CdS nanorods. The possible reason of low photocurrent and high V_{oc} is maybe due to the presence of ligand in the nanocrystals.

© 2009 Elsevier B.V. All rights reserved.

1. Introduction

In recent years, semiconductor nanowires have been increasingly studied as a potential material for future electronic applications due to their attractive size-dependent physical and electronic properties [1–8]. Nanowires with small diameters (less than 5 nm) are attractive both as interconnect and critical device elements because the bandgap and other physical properties strongly depend on their diameter [9]. It has recently been proposed that nanowires with such small diameters are ideal for the fabrication of nanowire MOSFETs for studying true one dimensional transport at room temperature. Furthermore, nanowires have the potential to improve charge transfer and charge collection efficiency in photovoltaic devices [7,10,11]. This is because nanowires can easily form an interconnected network in a conducting polymer thin film when prepared using spin-coating. The network structure may enhance exciton separation, diffusion of free charges and charge collection efficiency [12].

A variety of methods such as the vapour–liquid–solid (VLS) method, solution–liquid–solid (SLS), the hydrothermal method and the hot coordinating solvents method using tri-*n*-octylphosphine oxide (TOPO) and trioctylphosphine (TOP) have been employed to synthesize semiconductor nanowires recently. Growth of nanowires via VLS often suffers from the requirements of high temperature, special conditions and complex procedures. In general, the size and aspect ratio distributions of these nanowires are difficult to control

[13]. Bottom-up approaches such as those using surfactants as the regulating agents are very effective for the synthesis of one-dimensional nanostructures because of their high efficiency, controllability and simplicity. Alivisatos et al. and Peng et al. have successfully developed a high temperature (around 300 °C), non-aqueous based method to synthesize cadmium chalcogenide nanocrystals with different shapes, such as dots, rods and tetrapods [14–18]. This method can generate well-defined nanodots and rods due to the separation of the nucleation and growth stages [19,20]. However, it is still a challenge to synthesize nanowires and solution based synthesis of nanowires is rarely reported [21].

Pradhan et al. reported the synthesis of cadmium selenide (CdSe) nanowires, in which attachment occurred in specific orientations via a loose and weak interaction between the nanoclusters [21]. Very recently, Kang et al. reported their research on preparing cadmium sulphide (CdS) nanowires using tetradecylphosphonic acid as a ligand. They only studied the effect of temperature on the morphology of the nanowires [22] and the nanowires they produced are mixed with many dots and branches. On top of that, their synthesis is rather complicated because it requires a two step heating process to prepare the Cd-complexes.

In this study, we report a simple route to synthesize high quality CdS nanowires. The ligand we used has a long alkyl chain – phosphonic acid–octadecylphosphonic acid (ODPA). Increasing the length of the alkyl chain reduces the diffusion rate and decreases the reactivity which we believed would improved control over the morphology of the nanocrystals. Our preliminary results showed that ODPA is better at controlling the morphology than dodecylphosphonic acid or hexylphosphonic acid [23].

* Corresponding author. Fax: +65 6790 9081.

E-mail address: ymlam@ntu.edu.sg (Y.M. Lam).

We also studied the effect of the timing of the precursor injection on the morphology of nanocrystals. Finally, the potential applications of these highly dispersible and high aspect ratio nanowires in hybrid nanowire/polymer solar cells using a blend of poly[2-methoxy-5-(2'-ethylhexyloxy)-1,4-phenylene vinylene] (MEH-PPV) and our CdS nanowires will be investigated.

2. Experimental details

2.1. Synthesis of nanocrystals

Triethylphosphine oxide (TOPO) and poly[2-methoxy-5-(2'-ethylhexyloxy)-1,4-phenylene vinylene](MEH-PPV) were purchased from Sigma-Aldrich. Triethylphosphine (TOP) and cadmium oxide were purchased from Fluka. Octadecylphosphonic acid (ODPA) and sulphur were purchased from Polycarbon Inc. and Chemicon respectively. PEDOT:PSS (Poly(3,4-ethylenedioxythiophene):poly(styrenesulfonate)) was purchased from Bayer AG. The CdS nanowires were prepared using a modified Peng's procedure for cadmium chalcogenide nanocrystals [20]. 128 mg of CdO, 0.668 g of ODPA and 3.00 g of TOPO were added to a 25 ml three-neck flask equipped with a condenser and a thermocouple adapter. The flask was then filled with N₂ and the temperature was gradually raised to 330 °C to dissolve the CdO. The temperature was then lowered to 310 °C and stabilised, and a solution of 32 mg sulphur in 2.0 g TOP was injected using multiple injections (4 times at 2 min intervals). After the final injection, the temperature of the reaction mixture was maintained at 310 °C for further growth. The reaction was terminated by stopping the heating.

2.2. Device fabrication

Hybrid solar cells were fabricated using a structure consisting of ITO/PEDOT:PSS/MEH-PPV:CdS nanowires blend/Al layers. A layer of PEDOT:PSS was spin-coated onto the etched ITO glass and dried at 120 °C for 20 min. After the synthesis, CdS nanocrystals were dispersed in 20 ml pyridine and stirred under reflux for 4 days, allowing for ligand exchange. Nanocrystals were then precipitated with n-hexane and then redissolved in pyridine. The above process is repeated one more time. After ligand exchange, the nanocrystals and MEH-PPV were dissolved in pyridine separately. A mixture of the nanocrystals and MEH-PPV with 70% nanocrystal loading was prepared. The mixture was spin-coated on top of the dried PEDOT:PSS and dried at 130 °C for 30 min. Finally, aluminum was evaporated on top of the film.

2.3. Characterization

Transmission electron microscopy (TEM) was carried out using a JEOL 2010 microscope fitted with a LaB₆ filament and an acceleration voltage of 200 kV. Ultraviolet-visible (UV-Vis) absorption and photoluminescence (PL) spectra of the nanocrystals were obtained using a Shimadzu UV2501PC spectrophotometer and a Shimadzu RF-5301 PC fluorometer respectively. The excitation wavelength for the PL test was 350 nm. The ligand content of nanocrystals studied using a TA instruments Q500 thermogravimetric analyzer (TGA) from ambient to 650 °C at the rate of 10 °C min⁻¹ under nitrogen atmosphere, with a gas flow of 60 ml min⁻¹. Photocurrent measurements were carried out using a 150 W xenon lamp with an air-mass (AM) 1.5 filter. The optical power on the sample was 100 mW cm⁻². Current-voltage measurements (*I*-*V* curve) were conducted in ambient atmosphere.

3. Results and discussion

3.1. Synthesis and characterization of the nanocrystals

The monomer concentration in the solution is an important factor that influences the morphology of the resulting nanocrystals. In this

study, we investigated the effect of precursor injection processes on the morphology of nanocrystals. Fig. 1a shows a TEM image of self-aligned nearly monodisperse CdS nanorods prepared with an interval between precursor injections of more than 5 min. The aspect ratio of the nanowires is around 10 and their diameter is 3.5 nm. However, decreasing the interval between the precursor injections to around 2 min can lead to a great increase in the aspect ratio of nanocrystals.

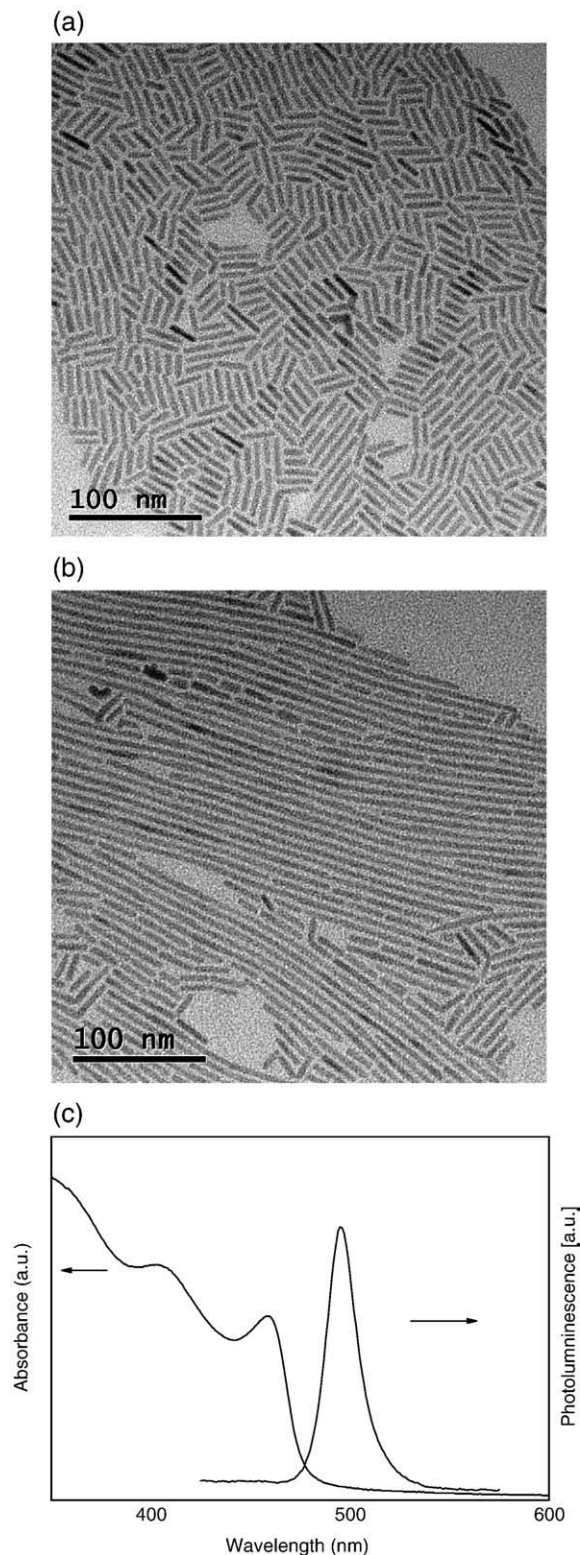


Fig. 1. Bright-field TEM images of CdS nanocrystals: (a) nanorods, (b) nanowires and (c) UV-Vis absorption and PL spectra of the CdS nanowires shown in b.

Fig. 1b is TEM image showing well aligned CdS nanowires prepared with a shorter injection interval. The aspect ratio varies from 10 to 170 and the diameter is about 3.6 nm. A possible explanation for the change in aspect ratio is that multiple injections replenish the monomer concentration regularly and hence provide a relatively stable growth environment [20]. Thus, after the nucleation stage, the presence of a high monomer concentration maintains the anisotropic growth regime for a longer time, resulting in a higher aspect ratio. When the precursor injection interval is increased, the monomer concentration is reduced and the growth environment became more variable. This gives rise to several nucleation and growth periods and thus the anisotropic growth necessary for high aspect ratio is not present, resulting in low aspect ratio rods.

Fig. 1c shows the UV–Vis absorption and PL spectra taken from the CdS nanowires shown in Fig. 1b. The sharp peak in the UV–Vis spectrum centered at around 460 nm indicates a nearly monodisperse diameter. As the long axis (length direction) of the nanowires is beyond the confinement regime, the excitation peak only depends on the short axis (diameter) of the nanowires [24,25]. The peak in the PL spectrum (Fig. 1c) at 495 nm arises from band-edge emission and is blue-shifted by 22 nm from the bulk CdS value at 517 nm due to quantum confinement. The sharpness of this PL peak is further evidence that the samples are monodisperse in diameter. It is also thought that the strong PL intensity from the CdS nanowires can be attributed to their high crystallinity [26,27]. Fig. 2 is a HRTEM image of several nanowires showing this region to be single crystalline with no stacking faults. However, there exists a small quantity of branched or bended structures as shown in Fig. 1b. These structures are often observed in the synthesis of II–VI anisotropic nanocrystals [14,19,20]. The stacking faults can be observed in the regions where the direction of the wires changed. The spacing of the lattice fringes along the length of the nanowires was measured to be about 0.337 nm, corresponding to the (002) lattice plane spacing of wurtzite CdS (0.336 nm). This indicates that nanowire growth along the [001] direction is preferred, which is agreement with results from other groups [28–31].

3.2. Hybrid photovoltaic devices

In recent years, solar cells have drawn great attention as candidates for clean and renewable power [7,32]. Due to their high electron mobility and tunable absorption spectra, nanocrystals have a potential to improve the efficiency of photovoltaic devices [10,33]. Currently, nanodots, nanorods and tetrapod-shaped nanocrystals have been used as electron acceptors in hybrid nanocrystal/polymer solar cells

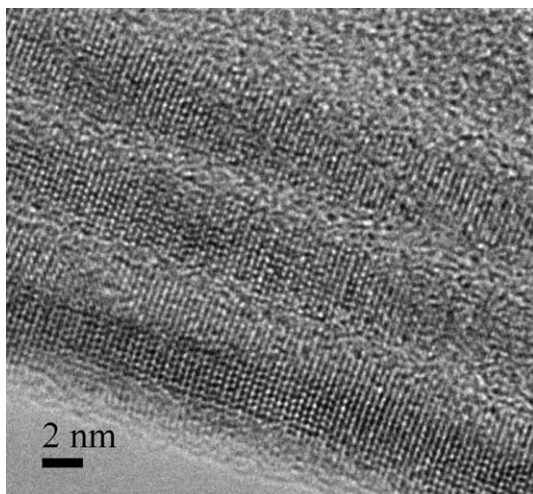


Fig. 2. High-resolution TEM image of several CdS nanowires.

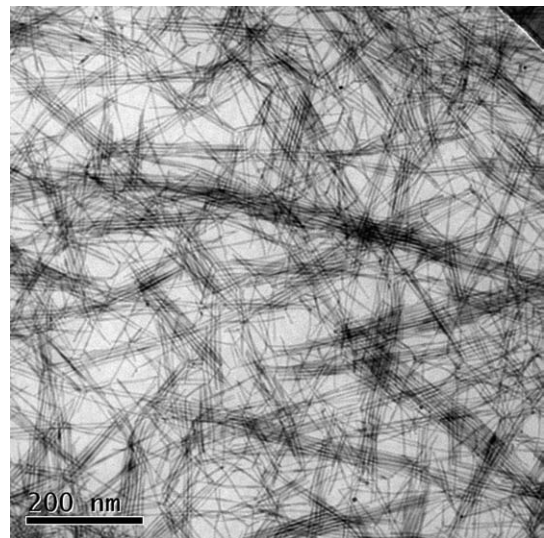


Fig. 3. Bright-field TEM image showing CdS nanowires dispersed in MEH-PPV.

[10,33–36]. It has been suggested that increasing the aspect ratio of the nanocrystals can enhance the charge transfer and further improve the performance of these devices [10,33]. Our CdS nanowires exhibit a high degree of dispersibility and have aspect ratios as high as 170. They are thus good candidates for improving the efficiency of photovoltaic devices.

Fig. 3 is a TEM image showing our nanowires in a polymer matrix. It can be seen that the nanowires form an interconnected network. It is thought that an active layer with a more intimate mixture can increase the amount of interaction between the conducting polymer chain and inorganic crystals [37]. This network structure can help in the exciton separation, the diffusion of free charges and the charge collection efficiency [12]. We thus investigate here the photovoltaic properties of hybrid solar cells made from our nanorods and nanowires blended with MEH-PPV.

Fig. 4 shows the UV–Vis absorption spectra from thin film blends of CdS nanocrystals/MEH-PPV and CdS nanowires/MEH-PPV. It can be seen that the absorption range of the thin film blend is wider than that of the pure MEH-PPV ($\lambda = 500$ nm). This indicates that CdS nanocrystals and MEH-PPV have complementary absorption spectra in the visible region [34]. Fig. 4 also shows that the blend film has good absorption capability. *I*–*V* curves from CdS nanowire and nanorod devices are presented in Fig. 5a–b. It is surprising that the maximum open-circuit voltage (V_{oc}) is 1.17 V for nanorods and 1.24 V for

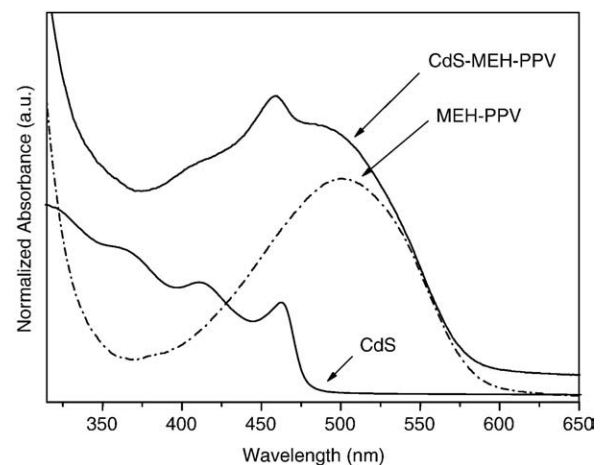


Fig. 4. UV–Vis absorption spectra from thin film blend of CdS nanorods and CdS nanowires with MEH-PPV.

nanowires containing devices. A possible reason can be proposed based on the TGA results which will be discussed below.

Compared to the nanorod blend, a two-fold increase in the short circuit photocurrent (I_{sc}) is found for the CdS nanowire blend. This resulted in a three-fold improvement in the overall power conversion efficiency for the nanowire blend from 0.01% to 0.03% under 100 mW cm^{-2} illumination. This result is consistent with Huynh et al.'s proposal that increasing the aspect ratio of the nanocrystals can enhance the charge transfer and improve the performance of the devices [10,33]. It was also found in our study that when the optical power is decreased to 50 mW cm^{-2} , the efficiencies of both devices are increased by 1.8 times. Despite the good absorption spectrum for our devices as shown in Fig. 4, the efficiency reported here is lower than that reported by others using same materials [38,39]. For example, Kang et al. reported an efficiency of 0.6% with well-aligned CdS nanorods/MEH-PPV solar cells [38]. Very recently, Wang et al. reported an even higher efficiency of 1.17% using multi-armed CdS nanorods/MEH-PPV solar cells [39]. The main reason for the comparably low efficiency of our devices is our low I_{sc} . In general, I_{sc} is affected by optical absorption properties, the thickness of active layer, the interface and the band-gap matching of the materials [12,40].

Fig. 6 shows the TG curves of TOPO, ODPA, CdS nanocrystals before ligand exchange, after the 1st and 2nd ligand exchange. It can be seen that the ligand capped nanocrystals is mainly ODPA, not TOPO as reported previous by other group [33]. The ligand exchange is found to be an efficient way to remove TOPO on the surface of nanocrystals. After

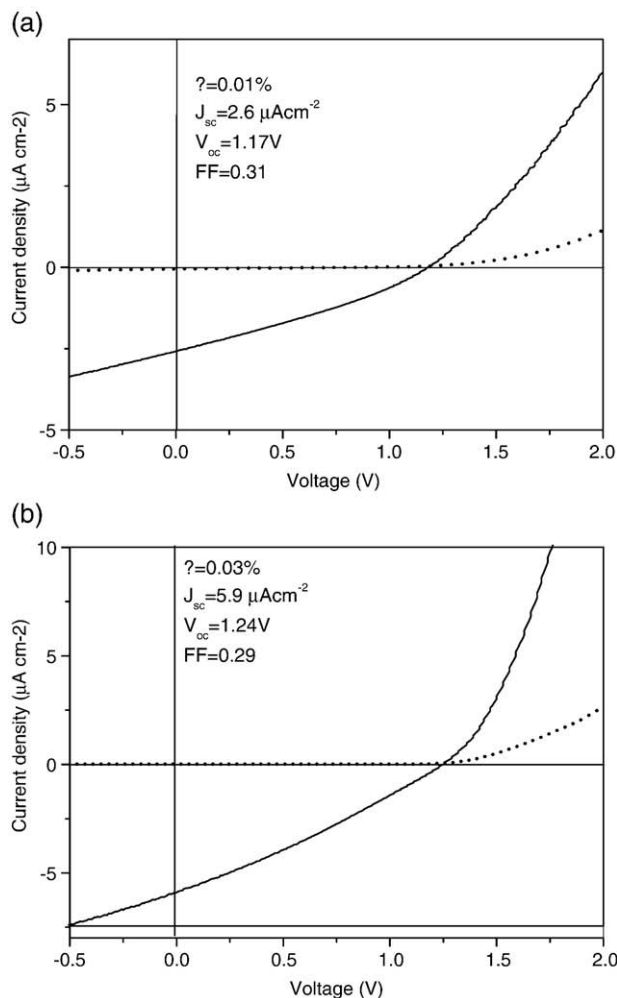


Fig. 5. I–V curves from photovoltaic devices made from (a) CdS nanorods/MEH-PPV and (b) CdS nanowires/MEH-PPV in the dark (dotted line) and under an illumination of 100 mW cm^{-2} (solid line).

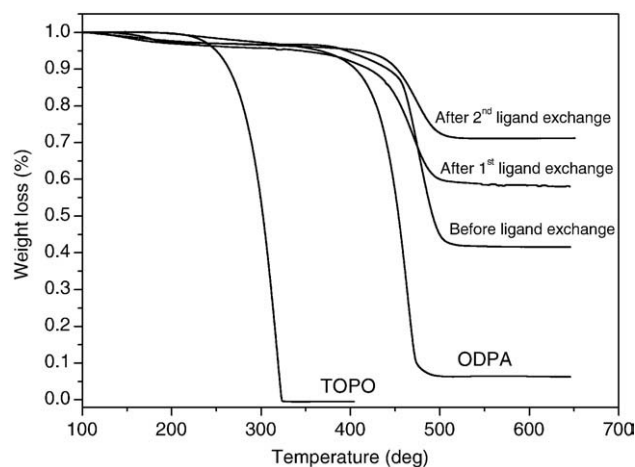


Fig. 6. TG curves of TOPO, ODPA, CdS nanocrystals before ligand exchange, after the 1st and 2nd ligand exchange, respectively.

the 1st ligand exchange with pyridine, the ligand content decreases from 59% to 42% in weight as shown in Fig. 6. In this study, we found even after the 2nd ligand exchanges, there is still about 29% ODPA in the nanocrystals. These ODPA can either be directly attached onto the surface of the nanocrystals or can exist as unreacted Cd–ODPA complexes mixed with nanocrystals. It is reported that the conversion of trialkylphosphine chalcogenide is about 80% under anhydrous conditions [19,41]. Therefore we can assume that the reason for the relatively low photocurrent and high V_{oc} is probably due to the present of ODPA in the nanocrystals which leads to a high resistance. We further studied the spectra response of devices and found that the maximal quantum efficiency (EQE) value is about 3% (at 490 nm) for the devices based on CdS nanowires/MEH-PPV. The relatively low EQE can tell us the efficiency of charge transport is poor [10]. In order to improve the performance, we need to improve the surface state of the nanocrystals. Small molecular organics such as ODPA can trap charge carriers, thus reducing the efficiency of charge separation and transportation [10,42].

4. Conclusions

In summary, high solubility monodisperse CdS nanowires were synthesized in solution. Their aspect ratio ranged from 10 to 170 and their diameter was 3.6 nm. It was found that varying the interval between the multiple injections of precursor had a great impact on the aspect ratio of the nanocrystals formed. A possible explanation is that a suitable interval between the injections can provide a relatively stable growth environment. The presence of a high monomer concentration after nucleation can maintain the anisotropic growth regime for a long time, resulting in a higher aspect ratio. The sharp peaks in both UV–Vis absorption and PL spectra indicate that the diameter distribution is nearly monodisperse. The photovoltaic properties of devices containing blends of the different nanocrystals with MEH-PPV were studied. The efficiency of these devices increased from 0.01% to 0.03% when nanowires were used in the blend instead of nanorods. This result proves that increasing the aspect ratio of the nanocrystals can enhance the charge transfer and further improve the performance of the devices. The main reason for their comparably low efficiency comes from their low I_{sc} . Future work will focus on improving the surface states of the nanocrystals as well as optimizing parameters such as annealing conditions and the nanocrystals loading.

Acknowledgments

This work is supported by the Science and Engineering Research Council, Agency for Science, Technology and Research (A*STAR), Singapore.

References

- [1] J.B. Baxter, E.S. Aydil, *Appl. Phys. Lett.* 86/5 (2005) 053114.
- [2] Y. Huang, X. Duan, Y. Cui, L.J. Lauhon, K.-H. Kim, C.M. Lieber, *Science* 294/5545 (2001) 1313.
- [3] A. Javey, S.W. Nam, R.S. Friedman, H. Yan, C.M. Lieber, *Nano Lett.* 7/3 (2007) 773.
- [4] M. Law, L.E. Greene, J.C. Johnson, R. Saykally, P. Yang, *Nat. Mater.* 4/6 (2005) 455.
- [5] W. Lu, C.M. Lieber, *Nat. Mater.* 6/11 (2007) 841.
- [6] A. Shik, H.E. Ruda, I.G. Currie, *J. Appl. Phys.* 98/9 (2005) 094306.
- [7] B. Tian, X. Zheng, T.J. Kempa, Y. Fang, N. Yu, G. Yu, J. Huang, C.M. Lieber, *Nature* 449/7164 (2007) 885.
- [8] Z.L. Wang, J. Song, *Science* 312/5771 (2006) 242.
- [9] G. Liang, J. Xiang, N. Kharche, G. Klimeck, C.M. Lieber, M. Lundstrom, *Nano Lett.* 7/3 (2007) 642.
- [10] W.U. Huynh, J.J. Dittmer, A.P. Alivisatos, *Science* 295/5564 (2002) 2425.
- [11] Y. Zhang, L.W. Wang, A. Mascarenhas, *Nano Lett.* 7/5 (2007) 1264.
- [12] H. Hoppe, N.S. Sariciftci, *J. Mater. Res.* 19 (2004) 1924.
- [13] J.D. Holmes, K.P. Johnston, R.C. Doty, B.A. Korgel, *Science* 287/5457 (2000) 1471.
- [14] L. Manna, E.C. Scher, A.P. Alivisatos, *J. Am. Chem. Soc.* 122/51 (2000) 12700.
- [15] X.G. Peng, L. Manna, W. Yang, J. Wickham, E. Scher, A. Kadavanich, A.P. Alivisatos, *Nature* 404/6773 (2000) 59.
- [16] W.W. Yu, Y.A. Wang, X. Peng, *Chem. Mater.* 15/22 (2003) 4300.
- [17] L. Manna, D.J. Milliron, A. Meisel, E.C. Scher, A.P. Alivisatos, *Nat. Mater.* 2/6 (2003) 382.
- [18] D. Battaglia, J.J. Li, Y.J. Wang, X.G. Peng, *Angew. Chem. Int. Ed.* 42/41 (2003) 5035.
- [19] Z.A. Peng, X. Peng, *J. Am. Chem. Soc.* 123/7 (2001) 1389.
- [20] Z.A. Peng, X. Peng, *J. Am. Chem. Soc.* 124/13 (2002) 3343.
- [21] N. Pradhan, H. Xu, X. Peng, *Nano Lett.* 6/4 (2006) 720.
- [22] C.C. Kang, C.W. Lai, H.C. Peng, J.J. Shyue, P.T. Chou, *Small* 3/11 (2007) 1882.
- [23] L.F. Xi, W.X.W. Tan, C. Boothroyd, Y.M. Lam, *Chem. Mater.* 20/16 (2008) 5444.
- [24] L.F. Xi, Y.M. Lam, *J. Colloid Interface Sci.* 316/2 (2007) 771.
- [25] L.F. Xi, Y.M. Lam, Y.P. Xu, L.J. Li, *J. Colloid Interface Sci.* 320/2 (2008) 491.
- [26] Z. Tang, N.A. Kotov, M. Giersig, *Science* 297/5579 (2002) 237.
- [27] R. Venugopal, P.I. Lin, C.C. Liu, Y.T. Chen, *J. Am. Chem. Soc.* 127/32 (2005) 11262.
- [28] M. Bashouti, W. Salalha, M. Brumer, E. Zussman, E. Lifshitz, *Chem. Phys. Chem.* 7/1 (2006) 102.
- [29] J.H. Zhan, X.G. Yang, D.W. Wang, S.D. Li, Y. Xie, Y. Xia, Y. Qian, *Adv. Mater.* 12/18 (2000) 1348.
- [30] Y. Long, Z. Chen, W. Wang, F. Bai, A. Jin, C. Gu, *Appl. Phys. Lett.* 86/15 (2005) 153102.
- [31] J. Lee, *Thin Solid Films* 451–452 (2004) 170.
- [32] N.S. Lewis, *Science* 315/5813 (2007) 798.
- [33] W.U. Huynh, J.J. Dittmer, W.C. Libby, G.L. Whiting, A.P. Alivisatos, *Adv. Funct. Mater.* 13/1 (2003) 73.
- [34] Y. Zhou, Y. Li, H. Zhong, J. Hou, Y. Ding, C. Yang, Y. Li, *Nanotechnology* 17/16 (2006) 4041.
- [35] I. Gur, N.A. Fromer, C.P. Chen, A.G. Kanaras, A.P. Alivisatos, *Nano Lett.* 7/2 (2007) 409.
- [36] A. Martíá, N. López, E. Antolína, E. Cánova, C. Stanleyb, C. Farmerb, L. Cuadrac, A. Luque, *Thin Solid Films* 511–512 (2006) 638.
- [37] C.J. Brabec, *Sol. Energy Mater. Sol. Cells* 83/2–3 (2004) 273.
- [38] Y. Kang, D. Kim, *Sol. Energy Mater. Sol. Cells* 90/2 (2006) 166.
- [39] L. Wang, Y. Liu, X. Jiang, D. Qin, Y. Cao, *J. Phys. Chem. C* 111/26 (2007) 9538.
- [40] J. Rostalski, D. Meissner, *Sol. Energy Mater. Sol. Cells* 63/1 (2000) 37.
- [41] H. Liu, J.S. Owen, A.P. Alivisatos, *J. Am. Chem. Soc.* 129 (2007) 305.
- [42] H. Zhong, Y. Zhou, Y. Yang, C. Yang, Y. Li, *J. Phys. Chem. C* 111/17 (2007) 6538.